ingegneria sismica
International Journal of Earthquake Engineering
Anno XLIII - Num. 1 - 2026

Data processing method for long-term monitoring of weak environmental signals based on virtual instrument technology

Xuejie Wei[1,*], *Wanjun Li*[1] *and Yueqiang Chu*[1]

[1] School of Electronic and Control Engineering, North China Institute of Aerospace Engineering, Langfang, Hebei, 065000, China

SUMMARY: *In this paper, virtual instrument is used as a development tool to explore the path of accurate monitoring and data processing of signals in a weak environment. Based on the dynamic characteristics of the frequency of the received signal to generate the local carrier and spread spectrum sequence, frequency mixing, code sequence matching received signals, match the results of multi-bit non-coherent cumulative to improve the capture sensitivity, proposed multi-bit cumulative dynamic code sequence matching method. And based on the weak environmental signal monitoring needs, using sample point screening for weak signal digital averaging, improve the signal-to-noise ratio of the target signal, build a weak environmental signal monitoring system. The overall root mean square error of the weak environmental signal monitoring system after incorporating the highly dynamic spread spectrum signal capture scheme remains within the interval of (0.05,0.1) in 50 experiments, which is both stable and effective.*

KEYWORDS: *multi-bit accumulation; dynamic code sequence matching; virtual instrumentation; sample point sampling; weak environmental signal monitoring*

1 Introduction

With the development of science and technology, all kinds of weak environmental signals are more and more emphasized by people. Weak environmental signals are widely present in the development of modern science and technology, especially in the fields of medicine, biomedicine, environmental monitoring, geophysics, precision instrument manufacturing, etc., and its monitoring is of great significance for human production and life [1-3]. For example, in the field of geophysical exploration, environmental signal monitoring can also be used to search for resources such as oil and natural gas, which can help in energy production. In the field of medical imaging, weak environmental signal monitoring can monitor the focal area in real time and efficiently, and accurately locate and analyze the causes of diseases [4]. The weak characteristics of weak environmental signals can be roughly learned from two aspects: one aspect refers to the detection of microvolt, nanovolt, or even picovolt-level voltage signals, which all have very small signal amplitudes; the other aspect is that, compared with the noise signals, researchers prefer to obtain signals with smaller amplitudes (e.g., weak light, small displacements, microvibrations, microstrains, and microtemperature differences, etc.), and a large amount of information exists in these weak signals, which can be used to provide decision support in several application areas [5-9].

The traditional monitoring of weak environmental signals is manually measured by human

*18031630662@163.com
https://doi.org/10.65102/is2026098 Published: 30 April, 2026

beings, which is not real-time and sustainable, and the accuracy is difficult to guarantee due to various errors. In addition, manual measurements require testers to master multiple instrument operation guidelines, the data between instruments are independent of each other, and the quality of data processing is flawed; and batch signal monitoring is inefficient and costly [10-12]. Based on this, it highlights the urgency of developing an automated, high-quality, and efficient data processing tool for weak environmental signal monitoring.

Virtual instrument technology as a new test instrument concept promotes the development of traditional measuring instruments towards digitalization, intelligence and modularization. It is the use of computers and high-performance modular hardware, combined with efficient and flexible software to complete a variety of test, measurement and automation applications [13]. Virtual instrumentation combines computer resources with instrument hardware and digital signal processing technology to transform the way manufacturers define instrument functions into the user's own definition of instrument functions, the user can be based on the needs of the test, their own design of the required instrument system, the use of one or more functions of the general module, call the different functions of the software module, the composition of different instrument functions, with the potential to become the processing of weak environmental signals technology [14-17].

Data processing for long-term monitoring of weak environmental signals involves signal acquisition, signal conditioning and processing. In the signal acquisition phase, Tang et al [18] designed a low-complexity capture algorithm for satellite-borne receivers to capture weak direct sequence spread spectrum signals, and achieved 90% detection rate in all three carrier-to-noise ratio environments. Deng et al [19] reported a novel signal acquisition algorithm based on partially matched filters, frequency compensation, block accumulation, and fast Fourier transform for intercepting frequencies in weak environmental signals, which has low computational load and high capture accuracy. Liu et al [20] used arrival time difference algorithm and receiver to locate and capture the weak signals of mobile communication respectively, introduced the multivariate orthogonal amplitude modulation technique to modulate the signal transmission pattern and constructed the signal feature classifiers, and identified the signals by combining the classifiers and information fusion techniques, the identification rate is higher than the traditional methods and the accuracy rate is also improved. Zhu et al [21] proposed a novel BeiDou weak signal acquisition algorithm in obstructed environments, which is realized by a circular shift algorithm, differential coherent integration module, and adaptive threshold detection with random noise power. Gao et al [22] developed a high-precision weak signal acquisition system that integrates several functional areas such as hardware acquisition circuit, driver circuit, and upper computer processing, and effectively acquires a high-precision signal of 0.5 volts DC signal.

In the weak signal conditioning and processing stage, Deng et al [23] proposed an adaptive bandwidth Fourier decomposition method based on Fourier spectral bandwidth optimization, empirical wavelet transform, and narrow-band characteristics for decomposing weak signal components from a multi-component signal processing environment. Wu et al [24] developed a digital receiver based on the concept of cumulative increase in receiver sensitivity, which can effectively improve the signal-to-noise ratio and reduce the number of real samples used to improve the detection efficiency of weak signals. Elango et al [25] incorporated a pre-filtering technique based on reduced-rank singular spectrum analysis in a weak signal receiver of a civil GPS system, which successfully eliminated the noise of the signal acquisition in weak environments, obtaining a detection probability of 96%. Wang et al [26] set up a novel guided wave array signal processing method for weak signal processing in long range detection, which mainly involves intercepting the covariance matrices of different time windows of some array signals and performing singular value decomposition to obtain the time of flight of the scattered

signals in the damaged region. The frequency domain cumulative averaging algorithm designed by Chen et al [27] can deal with improving the signal-to-noise ratio of weak vibration signals in distributed vibration sensing systems while reducing the low-frequency spectral variance, which makes the identification and localization of weak vibration signals more accurate. Liu et al [28] studied the wire rope weak signal processing method, using the flux leakage test and multi-step filtering technique was realized, the method of processing the signal can be obtained as high as 90.37 dB signal-to-noise ratio. Zhao and Jia [29] used a reweighted singular value decomposition strategy to denoise weak signals in a large number of noisy and interfering environments, and at the same time, strengthened the weak signal features so that the weak features could be highlighted. Zhang et al [30] applied a radial basis function-neural network to adapt the Kalman filter algorithm for extracting weak signals in a low signal-to-noise ratio environment, and the weak signal extraction at a signal-to-noise ratio of -10 dB remained successful.

Academic about the current status of the application of virtual instrumentation technology in the field related to the monitoring of weak environmental signals. Song et al [31] collected the induced electrical signals in the electromagnetic environment of a substation with the help of nickel-type data acquisition equipment and introduced a lock-in amplifier based on a virtual phase-intensive detector and digital filters to reduce the signal noise, so as to obtain the weak signals. Zhang et al [32] proposed a multi-channel weak eddy current signal detector based on virtual instrumentation and self-balancing techniques, with a single detection width of up to 56.00 mm and a detected coverage of up to 2.90 mm. Jiang and Cheng [33] constructed an online monitoring system for motor temperature through LoRa wireless communication and virtual instrumentation technology to collect data with temperature sensors, and after the data were converted into voltage signals under the temperature signal conditioning circuit, followed by filtering and heterodyne checking processing, and inputted into the upper computer, realizing the whole process from data collection to data conditioning and processing.

This paper firstly describes the components and concepts of virtual instrument technology to lay the foundation of research technology. Then it elaborates the mathematical operation of the non-coherent accumulation capture algorithm, the influence of large Doppler frequency on the non-coherent accumulation algorithm, and establishes the dynamic code sequence matching capture method. Subsequently, on the basis of the traditional digital averaging monitoring method, combined with the statistical characteristics of noise, the digital averaging algorithm of sample point sampling is proposed to form a weak environmental signal monitoring system. After that, the overall application effect of the weak environmental signal monitoring system is evaluated, and the high dynamic spread spectrum signal capture scheme is designed by combining the effect of delayed superposition capture experiment. Finally, we set up a comparison experiment between denoising effect and monitoring accuracy to verify the feasibility of the proposed monitoring system.

2 Components of a virtual instrument

The virtual instrument consists of three parts: data acquisition and control, data processing and analysis, and displaying the results, and its composition architecture is shown in Fig. 1. In traditional instruments, the functions of these parts are basically realized by the hardware; in virtual instruments, the first part is completed by the hardware, and the remaining two parts are completed by the software. The design of the virtual instrument develops in the direction of standardization and modularization, which makes the workload of the developer much less.

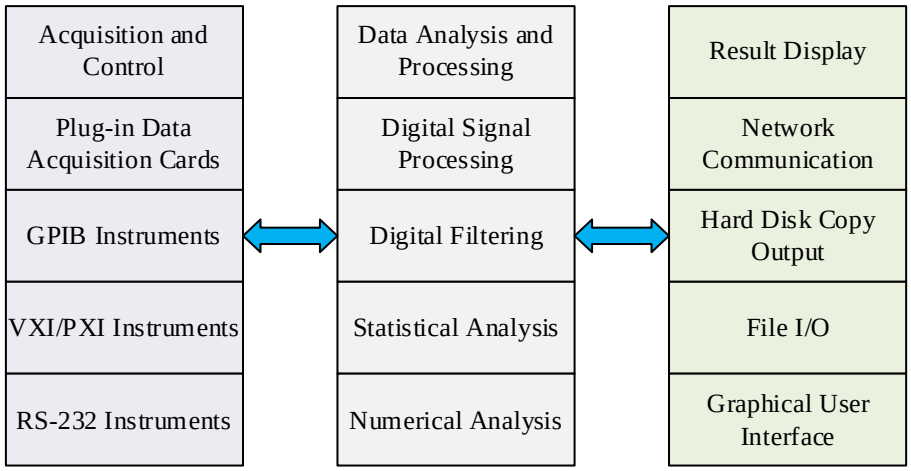

Figure 1: The composition of virtual instruments

In the virtual instrument test system, the core function is realized by the software, while the normal operation of the virtual instrument is ensured by the hardware. Usually the computer, sensors, signal conditioning circuits and signal acquisition components constitute the hardware part of the virtual instrument test system. Sensors convert various variables present in the real world into electrical signals. Signal conditioning amplifies, filters, synchronizes, and linearizes the electrical signals to enable the analog-to-digital converter to receive the signals. Data acquisition converts the obtained signal to A/D conversion. PC becomes a specific platform for virtual instrument software to run, and is the center of data acquisition and processing. The combination of these hardware can be optimized according to the needs of the way; the software part of the system is generally written in a special virtual instrument development language, and then through the network to achieve expansion. Software in the virtual instrument system occupies a central position, so that the computer has a signal acquisition, processing and results display instrument function.

The most important part of virtual instrument technology is software. Users can use a variety of programming tools to develop the required application software. The development language of virtual instrument system includes C language, VB, VC++ and other common program development language. However, designing a virtual instrument system with the above languages requires not only the design of the instrument panel, but also a lot of effort and time to write a large number of device drivers and control programs. For those engineering designers who are not very proficient in these general-purpose program programming languages, it takes a lot of time to complete the above work, slowing down the system development cycle. Therefore there are also some influential specialized virtual instrument development language and software, such as LabVIEW, LabWindows/CVI, Ez-Test, Tek-TNS platform software. Currently the popular virtual instrument integrated development tools are based on the U.S. National Instruments dedicated development platform LabWindows/CVI and LabVIEW.

LabWindows/CVI is a standard ANSIC development environment in the Windows environment, for developers familiar with the C language is prepared.LabVIEW is the use of graphical programming development software. These dedicated development platforms provide powerful soft panel design tools and data processing tools, and manufacturers also provide the corresponding drivers for hardware instruments, making the design process of virtual instruments simple. With the modularization and standardization of software development and various hardware driver software, the development process of virtual instrument software has become more convenient.

Virtual instrument technology opens up a whole new period of self-designed instruments,

providing a wide thinking space for designers of different levels. The progress of computer software and hardware technology is an important factor in determining the development of virtual instrument technology. Software is the focus of the realization of virtual instruments. Completing the determination of the basic hardware, the designer realizes different functions through different software programming to build a virtual instrument system with diverse performance. Therefore, it is necessary to consider how to improve the programming efficiency of the corresponding software. Through the use of LabVIEW's powerful graphical programming language can exponentially increase productivity.

3 Construction of a weak environmental signal monitoring system

3.1 Multi-bit cumulative dynamic code sequence matching method

3.1.1 Non-coherent cumulative capture algorithm

In order to realize signal capture in weak signal environments, coherent accumulation, incoherent accumulation, and differential coherent accumulation methods have been successively applied. Since the accumulation time of the coherent accumulation method is limited due to the presence of bit-hopping, and the differential coherent accumulation method is complicated to implement, typical high-sensitivity capture techniques usually use the non-coherent accumulation method to obtain the processing gain.

To realize the signal capture, the corresponding spread spectrum sequence is generated locally, and the correlation operation is performed with the down-converted baseband signal, and the correlation-processed baseband signal can be expressed as equation (1):

$$\begin{aligned} z(t_n) &= \frac{1}{2} AD(t_n) R(\Delta\tau) \sin c(\Delta\omega_D t_n) \\ &\quad \times \exp\left(-j\left(\Delta\omega_D t_n + \varphi\right)\right) + w(t_n), \\ n &= 1, 2, 3, \cdots \end{aligned} \tag{1}$$

where: t_n denotes the sampling time series; A is the signal amplitude; $D(t_n)$ denotes the baseband data taking the value of ± 1; $R(\cdot)$ is the autocorrelation function of the spreading sequence; $\Delta\tau$ is the code phase deviation of the locally replicated spreading sequence from the received one; $\sin c(\cdot)$ is the Singer function; $\Delta\omega_{\mathrm{D}}$ is the Doppler frequency difference between the locally replicated signal and the received signal; and φ is the initial phase of the carrier; $w(t_n)$ is the noise after the correlation operation. When $\Delta\tau$ and $\Delta\omega_{\mathrm{D}}$ are equal to 0, $z(t_n)$ obtains the maximum value.

Non-coherent accumulation means removing the phase information of the signal and accumulating only the amplitude information of the signal. The processing method is to sum the squares of the in-phase component $z_I(t_n)$ and the orthogonal component $z_Q(t_n)$ of the baseband signal $z(t_n)$ after the correlation process, and then accumulate them. The signal noncoherent cumulative detection statistic $P(t_n)$ is expressed as equation (2):

$$P(t_n)=\sum_{n=1}^{M}\left[\left(z_I(t_n)\right)^2+\left(z_Q(t_n)\right)^2\right] \tag{2}$$

where: M is the number of non-coherent accumulations. It can be seen that the incoherent accumulation eliminates the effect of bit-hopping in the squaring process and is more tolerant to the Doppler frequency difference $\Delta\omega_D$.

3.1.2 Large Doppler effect on incoherent accumulation

In the high-dynamic low-rate communication environment, on the one hand, the Doppler frequency and code rate of the high-dynamic signals have a large change, that is, the frequency characteristics and code phase characteristics of the signals change quickly; on the other hand, in order to improve the capture sensitivity of the spreading sequence, the use of multibit incoherent accumulation leads to a long data period of the low-rate data. Therefore, when performing highly dynamic low-rate signal capture, the frequency characteristics and code phase characteristics of the last few bits of multi-bit accumulation have changed compared to the first few bits. The $\Delta\tau$, $\Delta\omega_D$ increases, making the autocorrelation loss $R(\Delta\tau)$ larger. The correlation peaks after multi-bit separate correlation are shifted, resulting in a decrease in the incoherent cumulative gain and a decrease in the capture sensitivity. The phase variation of the multi-bit cumulative code is shown in Fig. 2.

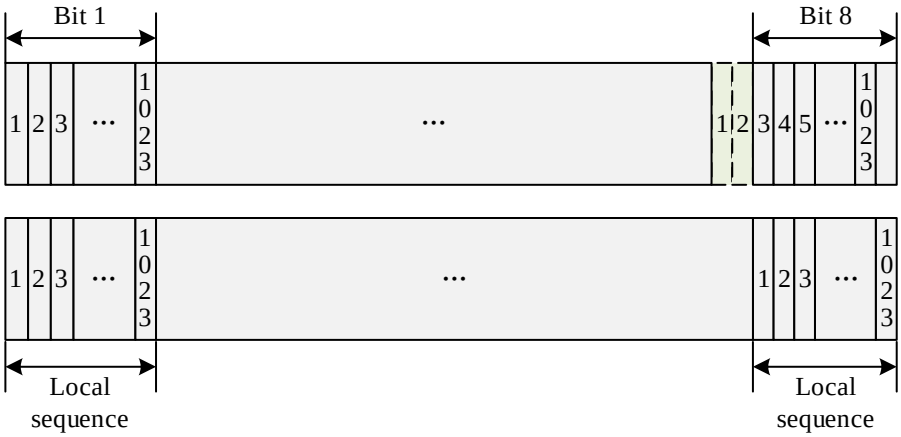

Figure 2: Phase characteristic variation of multi-bit cumulative codes

3.1.3 Dynamic Code Sequence Matching Capture Methods

With the dynamic code sequence matching technique, the local code sequence involved in matching is no longer a static spread spectrum code sequence, but a dynamic code sequence with the same Doppler frequency characteristics as the received signal. When the Doppler characteristics of the received signal change with the motion characteristics in real time, the local matching sequence has the same change characteristics. The instantaneous Doppler frequency of the received signal at the sampling moment t_n is expressed as equation (3):

$$f(t_n)=f_D+\frac{\partial f(t_n)}{\partial t}t_n \tag{3}$$

where: f_D is the initial Doppler frequency; $\frac{\partial f(t_n)}{\partial t}$ is the Doppler frequency change rate.

The local spread spectrum code has the same Doppler frequency dynamic characteristics, then the instantaneous spread spectrum code rate at the sampling moment is calculated as equation (4):

$$f_{CAD}(t_n) = f_{CA} + \frac{f(t_n)}{f_c} f_{CA} \tag{4}$$

where: f_{CA} is the initial spreading code rate; f_c is the carrier frequency. It can be seen that the spreading code rate under dynamic conditions is a quantity that changes according to the dynamic characteristics of the Doppler frequency of the signal.

During the signal capture process, when matching correlation and multi-bit incoherent accumulation of the spread spectrum sequence are performed, the rate of the local spread spectrum sequence is generated according to equation (4). When multi-bit incoherent accumulation is performed, the $\Delta\tau$ and $\Delta\omega_D$ between the local spread spectrum sequence and the received signal are almost zero, the autocorrelation loss is small, and the capture sensitivity is improved by performing multi-bit incoherent accumulation of the results of the correlation operation. The dynamic code sequence matching is shown in Fig. 3.

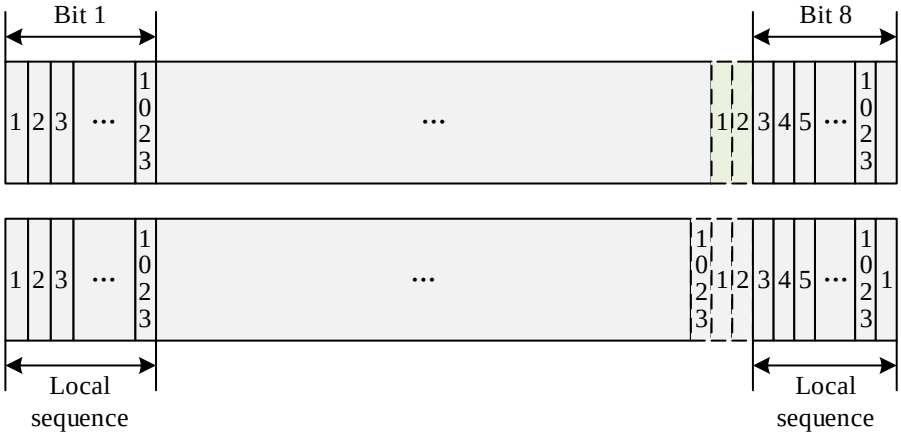

Figure 3: Dynamic code sequence matching

3.2 Sample point sampling average algorithm

Periodic deterministic signal under test, the signal period is T, the data acquisition card samples the signal under test with a sampling interval T_s, let $T = KT_s + hT_s\,(0 \le h < 1)$, there are two cases:

(1) If $h = 0$, the sampling rate is exactly an integer multiple of the signal frequency, each cycle has K sampling points and the samples collected in each cycle have the same phase.

(2) If $0 < h < 1$, the sampling rate is not an integer multiple of the signal frequency, resulting in the number of points sampled in each cycle is not exactly the same, the number of sample points for K or $K+1$. At this time for sample point screening, let the k sampling, the remaining time after the first $k-1$ sampling is $rem\left(\frac{(k-1)T}{T_s}\right)$, defined as equation (5):

$$\Delta t = rem\left(\frac{(k-1)T}{T_s}\right) + hT_s \tag{5}$$

There are: if $\Delta t < T_s$, the k th cycle has K sampling points, the same as in the case of $h = 0$; if $\Delta t \geq T_s$, the k th cycle has $K+1$ sampling points, and at this time, the $K+1$ th sampling point in this cycle is discarded so that this cycle has K sampling points. At this time the phase of each sampling value is not the same, the maximum phase difference is equation (6):

$$\frac{T_s}{T} 2\pi = \frac{T_s}{KT_s + hT_s} 2\pi = \frac{1}{K+h} 2\pi \tag{6}$$

Since $0 < h < 1$ and K is generally large, the phase difference is small and does not increase with the number of superpositions, and is uniformly distributed between $\left(-\frac{2\pi}{K}, \frac{2\pi}{K}\right)$, and when K is sufficiently large, the phase differences cancel each other out to some extent, and there is no error accumulation. The two cases are processed as described above so that each cycle has the same number of sampling points K in the absence of an external synchronization signal.

Let the input signal be equation (7):

$$f(t) = s(t) + n(t) \tag{7}$$

$s(t)$ is the periodic measured signal, U_s is the RMS value, $n(t)$ is the Gaussian white noise with zero mean and variance σ_x^2, and σ_x is the noise RMS value. The sample points of the same serial number in each cycle are averaged digitally superimposed, and the k th sampling is averaged by M th averaging output as equation (8):

$$u_0 = \frac{1}{M} \sum_{i=0}^{M-1} \left(t_k + iT\right) = \frac{1}{M} \sum_{i=0}^{M-1} s\left(t_k + iT\right) + \frac{1}{M} \sum_{i=0}^{M-1} n\left(t_k + iT\right) \tag{8}$$

where $k = 1, 2, \cdots, K$.

Since $n(t)$ has zero mean, so $\frac{1}{M} \sum_{i=0}^{M-1} n\left(t_k + iT\right) = 0$, the output signal RMS is equal to the input signal RMS.

The output noise RMS value is equation (9):

$$\frac{1}{M} \sqrt{\sum_{i=0}^{M-1} n^2\left(t_k + iT\right)} = \frac{1}{M} \sqrt{M\sigma_x^2} = \frac{\sigma_x}{\sqrt{M}} \tag{9}$$

The input signal-to-noise ratio is equation (10):

$$SNR_i = 20 \lg \frac{U_s}{\sigma_x} \tag{10}$$

The output signal-to-noise ratio is equation (11):

$$SNR_0 = 20\lg\frac{U_s}{\sigma_x/\sqrt{M}} \tag{11}$$

Then the signal-to-noise improvement ratio is equation (12):

$$SNR_0 - SNR_i = 20\lg\left(\frac{U_s}{\sigma_x/\sqrt{M}} \times \frac{\sigma_x}{U_s}\right) = 20\lg\sqrt{M} = 10\lg M \tag{12}$$

Based on the above analysis, the output signal-to-noise ratio is improved by $10\lg M\,(dB)$ after M times of averaging. In turn, the number of superimpositions required for digital averaging can be calculated according to equation (12).

4 Application and performance evaluation of weak environmental signal monitoring systems

In this chapter, the monitoring object is selected and the weak environmental signal monitoring system is applied to monitor the indoor environment to confirm the feasibility of the proposed monitoring system. Based on the experimental results of the delayed superposition capture scheme, a high dynamic spread spectrum signal capture scheme is designed to make up for the shortcomings of the proposed monitoring system in high dynamic spread spectrum signal capture. The overall performance of the improved weak environmental signal monitoring system is evaluated by denoising effect and monitoring accuracy experiments.

4.1 Effectiveness of the application of the monitoring system

A basement in Building I was selected as the monitoring object, and the indoor temperature, relative humidity, PM2.5 and formaldehyde were monitored during the time period of 19:30:00-19:50:00 on July 25, 2024, in which the indoor temperature, relative humidity, $PM_{2.5}$ and formaldehyde were monitored. According to the quality standard of indoor pollution, the upper limit of abnormal data value of temperature is set at 30°C, the upper limit of abnormal data value of humidity is set at 50%, and the upper limit of abnormal data value of $PM_{2.5}$ is set at 60 ppm, and the real-time part of the data of the monitoring system (19:30:00-19:31:00) is shown in Table 1.The temperature of the target of the monitoring returned by the system is in the interval of (21.0,23.0)°C. The relative humidity is in the interval of (45.0)°C. The relative humidity is in the interval of (45.0)°C, and the formaldehyde is in the interval of (45.5)°C, Relative humidity is in the range of (45.0,48.0)°C, $PM_{2.5}$ is in the range of (47.0,53.0)μg/m³, and formaldehyde is always 0.02mg/m³, which is in line with the daily situation of the monitoring object, and initially proves the feasibility of the designed monitoring system.

Table 1: Examples of real-time data in detection system

Time (s)	Temperature (°C)	Relative humidity (%)	$PM_{2.5}$ (μg/m³)	Formaldehyde (mg/m³)
19:30:00	22.3	46.9	48.5	0.02
19:30:06	22.9	46.3	48.8	0.02
19:30:12	21.1	45.7	48.1	0.02
19:30:18	21.4	47.6	52.5	0.02
19:30:24	22.9	47.8	51.5	0.02
19:30:30	21.6	46.4	50.8	0.02
19:30:36	22.5	46.8	51.7	0.02
19:30:42	21.6	45.3	52.3	0.02
19:30:48	22.2	47.3	48.9	0.02
19:30:54	22.7	45.9	51.7	0.02
19:31:00	22.4	46.4	51.2	0.02

4.2 Capture schemes for highly dynamic spread spectrum signals

4.2.1 Delayed Overlay Capture Scheme

Let the pseudo-code period of the spread spectrum signal in the system is 1080, the signal will be copied three times, in order to delay and then add up, so that only 360 times of search will be able to determine the approximate range of the phase of the received signal. After that, three more precise searches are made to determine the code phase of the received signal. If each code element is sampled only once, then even in the worst case, the total number of searches is only 365 to complete the capture, which is much smaller than the original 1080 searches, and the superimposed capture probability curve is shown in Figure 4.

Although the monitoring system in this paper can realize the search of multiple code phases at one time to speed up the capture speed, due to the superposition of signals, many cumulative signals are regarded as noise, causing a certain loss of signal-to-noise immunity. It can be seen that the monitoring system in this paper starts to converge at a SNR of -15, and after 3 superimpositions the convergence point falls at a SNR of -10, while after 5 superimpositions the probability of capture starts to converge to a probability of 1.0 at a SNR < -10.

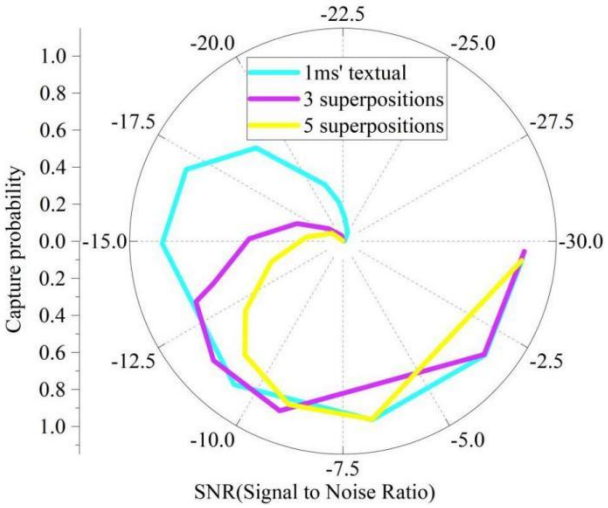

Figure 4: Probability Curve of Time-Delay-Addition Acquisition

4.2.2 Highly Dynamic Spread Spectrum Signal Capture Programs

For speeding up the search speed but does not reduce the demand for capture anti-jamming performance, this paper further proposes a specific capture scheme as follows: the received signal is delayed a times and superimposed with the original signal, consecutively take b segments of the periodic signal for capture, coherent accumulation of the b group of results obtained. If the peak is captured, the code phase of the received signal is determined to be in the a+1 code phase, and the a+1 code phase is captured. If the peak is not captured, the previous steps are repeated, and the selection of a and b can be adjusted according to the carrier dynamics as well as the signal-to-noise ratio of the received signal. The capture probability curves under the scheme are shown in Fig. 5 with the following simulation conditions: pseudo-code frequency of 1.03 Mchip/s, initial Doppler shift of 8000 Hz, acceleration of the object motion of 33 g, additive acceleration of 6 g, and the sampling rate of the received signal of 1.025 MHz. i.e., for each sampling of one codepoint, the FFT length is 256 points. Thus comparing Fig. 4 with Fig. 5, the proposed scheme is able to enhance the capture speed while significantly improving the signal capture probability under low signal-to-noise ratio conditions.

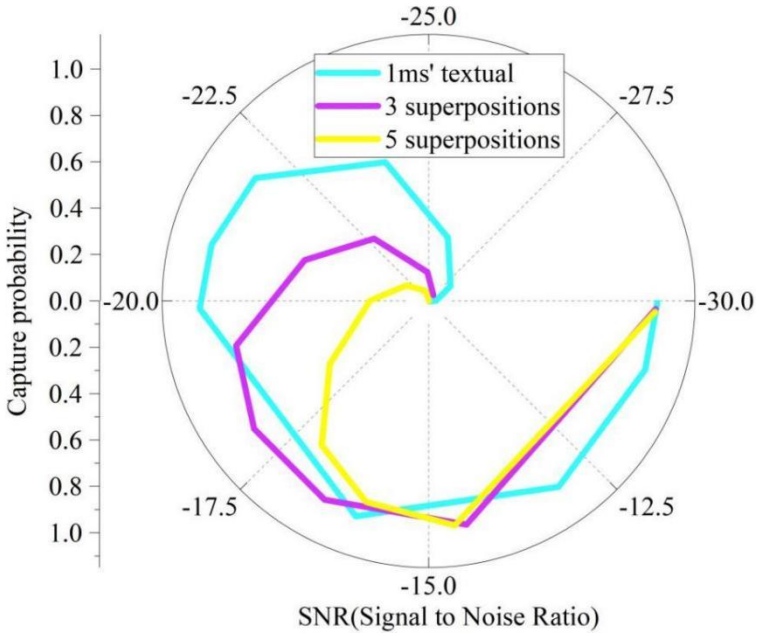

Figure 5: The capture probability curve of the improved scheme

4.3 Performance of the weak environmental signal monitoring system

4.3.1 Denoising effect

The signal in a basement of building I is selected for noise addition and denoising operation using the monitoring system proposed in this paper. The amplitude fluctuations of the signal before and after denoising are shown in Fig. 6(a)-(b). It can be seen that the signal amplitude after denoising by the method proposed in this paper basically coincides with the original noiseless signal amplitude (difference <0.01dB), which proves the effectiveness of this paper in removing the noise component in the signal.

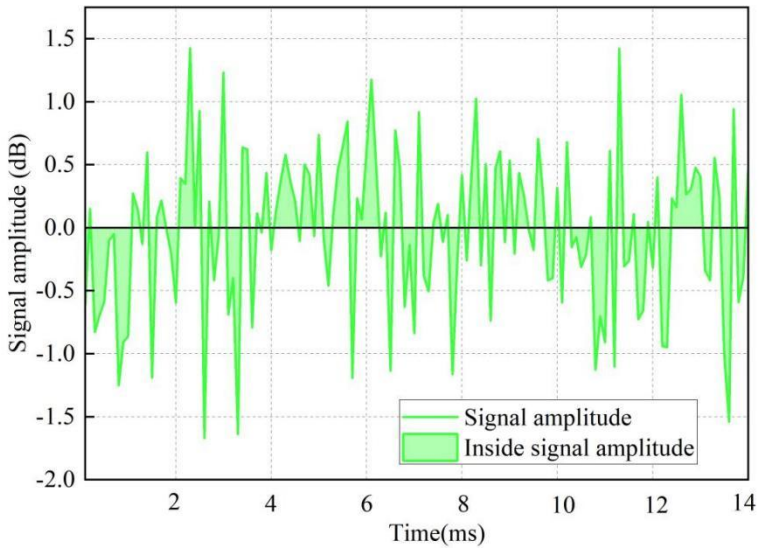

(a) Agitated signal

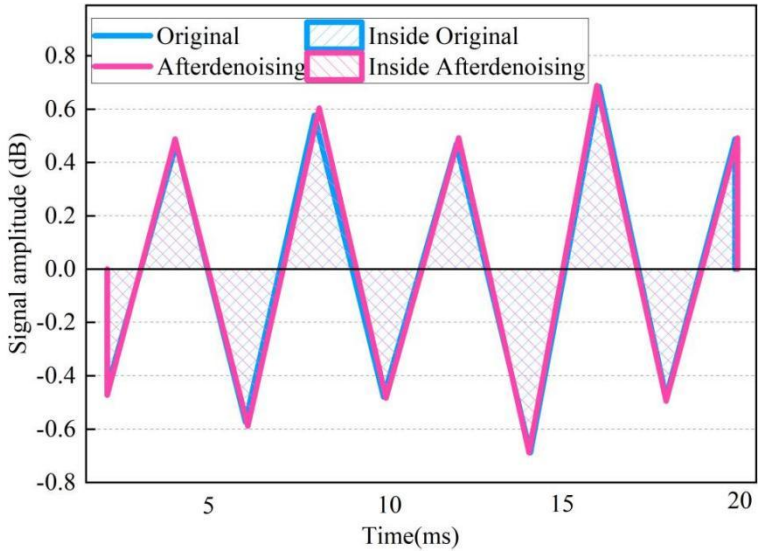

(b) The denoised signal by the method proposed in this paper

Figure 6: The amplitude fluctuation changes before and after denoising

4.3.2 Monitoring accuracy

The monitoring system in this paper is used to monitor the CO_2 volume fraction in a basement of building I from 16:00 to 14:00 the next day, and the comparison of the monitoring results with the validation data is shown in Fig. 7. The monitoring results of the system in this paper are highly consistent with the actual measurement data as a whole, and the deviation from the actual measurement data only occurs at 13:00 and 14:00 the next day, but it is controlled to be less than 300. Overall, the monitoring performance of the system in this paper is within a reasonable range of the monitoring accuracy of the experimental data, and can be put into practical use in the preliminary view.

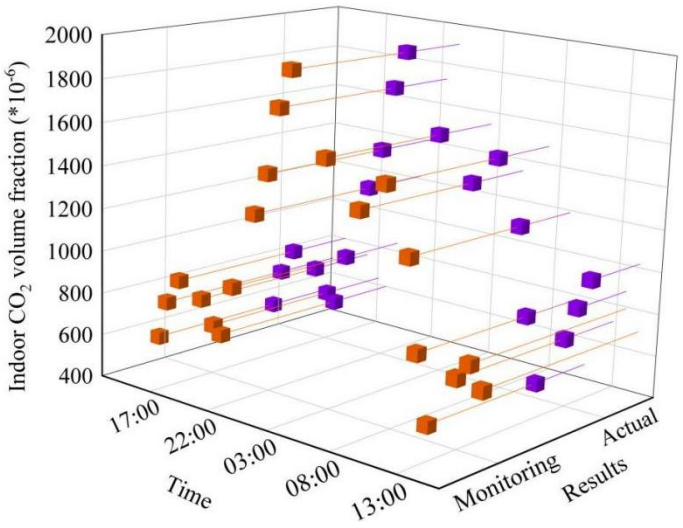

Figure 7: Monitoring results and actual measurement data

In order to further test the monitoring capability of (Z1) this paper's systematic method for weak environmental quality signals, (Z2) the dynamic monitoring method of formaldehyde in ambient air under the influence of indoor decoration and (Z3) the urban ecological environment monitoring method based on data mining are used as the control, and 50 experiments are conducted, and the comparison of the root mean square error performance of the results of the three methods is shown in Fig. 8, in which the root mean square error of the (Z1) this paper's systematic method for (Z1) The root mean square error of indoor environmental quality monitoring in this paper can be as low as 0.043, and the fluctuation amplitude is controlled within 0.05 in 50 experiments, and the overall root mean square error is within (0.05,0.1), which is not only of high monitoring accuracy but also of good robustness. (Z2)The RMSE of the dynamic monitoring method of formaldehyde in ambient air under the influence of indoor decoration was as high as 0.218>0.043, and the overall fluctuation was within a certain range. (Z3) The performance of the data mining-based ecological environment monitoring method for towns and cities is less satisfactory, and although the lowest root mean square error is 0.151, the overall fluctuation is large, with a difference of up to 0.18.

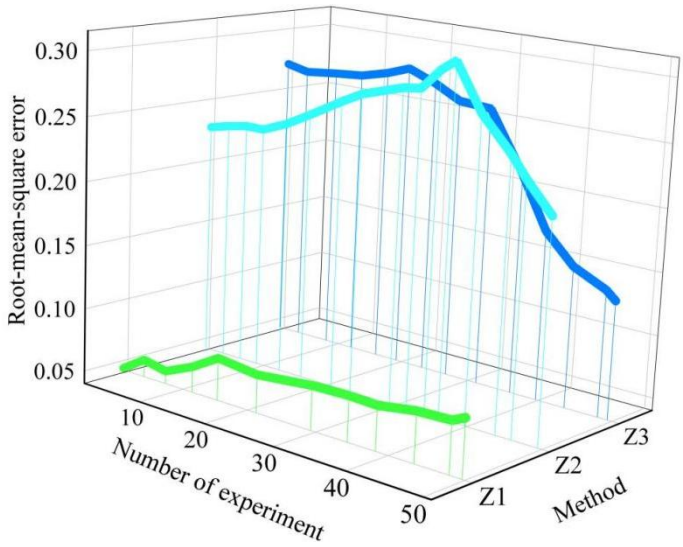

Figure 8: Experimental results of different methods

5 Conclusion

In this paper, for the signal characteristics and long-term monitoring needs of weak environment, based on virtual instrument technology, a dynamic code sequence matching method with multi-bit accumulation is designed, and a sample point sampling average algorithm is used for digital averaging of weak signals to construct a weak environment signal monitoring system. Meanwhile, for the anti-noise loss caused by multiple code phase search, a set of high dynamic spread spectrum signal capture scheme is specified, which enhances the capture speed and improves the signal capture probability under the condition of low signal-to-noise ratio at the same time.

The proposed weak environmental signal monitoring system is able to ensure that the amplitude of the denoised signal is highly consistent with the amplitude of the original noiseless signal (the difference is <0.01dB), and the root mean square error is controlled within the interval of (0.05,0.1) in 50 experiments, which provides an effective reference for the research on the accurate monitoring and fast capture of weak environmental signals.

Funding

This research was supported by the Hebei Provincial University of higher science and technology research project (No.: ZC2024051);

This research was supported by National Defense Innovation Fund Project of North China Institute of Aerospace Engineering (No. GFCXJJ-2023-03).

This work was supported by Key Project of North China Institute of Aerospace Engineering (No. ZD-2022-03);

About the Author

Xuejie Wei was born in Nanning, Guangxi, P.R. China, in 1981. She obtained a doctor's degree from La Consolacion University in Philippines. She works at the School of Electronic and Control Engineering, North China Institute of Aerospace Engineering. Her main research direction is Signal Acquisition and Virtual Instrument.

Wanjun Li was born in Chenzhou, Hunan, P.R. China, in 1988. He obtained a doctor's degree from La Consolacion University in Philippines. He works at the School of Electronic and Control Engineering, North China Institute of Aerospace Engineering. His main research direction is Analog Circuit Design and Signal Procession.

Yueqiang Chu was born in Bazhou, Hebei, P.R. China, in 1985. He obtained a master's degree from Hebei University of Technology in China. He works at the School of Electronic and Control Engineering, North China Institute of Aerospace Engineering. His main research direction is FPGA Development and Signal Acquisition.

References

[1] Carman, E. M., Fray, M., & Waterson, P. (2017). Weak signals in healthcare: A case study on community-based patient discharge. ndm, 314.

[2] Wang, R., Wang, J., Li, H., Cui, H., Tang, M., & Zhao, J. (2023). A study on the acquisition technology for weak seismic signals from deep geothermal reservoirs. Energies, 16(6), 2751.

[3] Augenblick, N., Lazarus, E., & Thaler, M. (2025). Overinference from weak signals and underinference from strong signals. The Quarterly Journal of Economics, 140(1), 335-401.

[4] Pereira, P. (2025). Quality control perspectives: weak signal detection to prevent clinical sensitivity failures in donors' screening. Transfusion and Apheresis Science, 104152.

[5] Song, Q., Li, H., Huang, J., Huang, P., Tan, X., Tao, Y., ... & Zeng, G. (2023). Weak signal extraction in non-stationary channel with weak measurement. Communications Physics, 6(1), 370.

[6] Sun, X., He, Y., Jin, T., Xie, J., Li, C., & Pang, J. (2023). Microseismic signal characteristics of the coal failure process under weak-energy and low-frequency disturbance. Sustainability, 15(19), 14387.

[7] Shi, L., Wang, J., Zhang, H., & Pan, L. (2025). A High-Performance and Sensitive Strain Sensor Based on MWCNT/Epoxy for Micro-Strain Monitoring of Steel Structure. Polymer Composites.

[8] Liu, B., Fu, Y., He, L., Geng, H., & Yang, L. (2023). Weak magnetic internal signal characteristics of pipe welds under internal pressure. Sensors, 23(3), 1147.

[9] Wang, G., Xing, F., Wei, M., & You, Z. (2017). Rapid optimization method of the strong stray light elimination for extremely weak light signal detection. Optics Express, 25(21), 26175-26185.

[10] Huang, M., Zhou, A., Wang, L., Wang, Y., & Qiu, G. (2023, August). Review of weak signals detection methods. In 2023 IEEE 16th International Conference on Electronic Measurement & Instruments (ICEMI) (pp. 98-104). IEEE.

[11] Wang, D., Song, Q., Li, H., Liu, Z., Huang, J., & Zeng, G. (2025). Enhanced Long-Distance Weak Signal Transmission Capabilities via Weak Measurement. Chinese Physics Letters.

[12] Yuan, J., Wang, Y., Peng, Y., & Wei, C. (2017). Weak fault detection and health degradation monitoring using customized standard multiwavelets. Mechanical Systems and Signal Processing, 94, 384-399.

[13] Nirubhanjali, R. V., & Soundharya, S. (2019). Virtual Instrumentation. International Journal of Engineering Research & Technology (IJERT), ISSN, 2278-0181.

[14] Melo, T. R., Neto, J. D. R., & Silva, J. J. (2021). Integration of virtual instrumentation in the teaching of data acquisition and interface systems course. IEEE Revista Iberoamericana de Tecnologias del Aprendizaje, 16(2), 154-160.

[15] Bonilla, D., Samaniego, M. G., Ramos, R., & Campbell, H. (2018). Practical and low-cost monitoring tool for building energy management systems using virtual instrumentation. Sustainable cities and society, 39, 155-162.

[16] El Hammoumi, A., Motahhir, S., Chalh, A., El Ghzizal, A., & Derouich, A. (2018). Low-cost virtual instrumentation of PV panel characteristics using Excel and Arduino in

comparison with traditional instrumentation. Renewables: wind, water, and solar, 5(1), 1-16.

[17] Kok, G., Wübbeler, G., & Elster, C. (2022). Impact of imperfect artefacts and the modus operandi on uncertainty quantification using virtual instruments. Metrology, 2(2), 311-319.

[18] Tang, P., Wang, S., Li, X., & Jiang, Z. (2017). A low-complexity algorithm for fast acquisition of weak DSSS signal in high dynamic environment. GPS Solutions, 21(4), 1427-1441.

[19] Deng, Z., Jia, B., Tang, S., Fu, X., & Mo, J. (2019). Fine frequency acquisition scheme in weak signal environment for a communication and navigation fusion system. Electronics, 8(8), 829.

[20] Liu, W. L., Jin, F., He, H. G., & Chen, Y. X. (2021, October). Weak Signal Acquisition and Recognition Method for Mobile Communication Based on Information Fusion. In International Conference on Advanced Hybrid Information Processing (pp. 62-73). Cham: Springer International Publishing.

[21] Zhu, Q., Chen, X., Zeng, J., & Shao, G. (2024, October). An Novel Beidou Weak Signal Acquisition Method in Obstructed Environments. In 2024 3rd International Symposium on Sensor Technology and Control (ISSTC) (pp. 243-246). IEEE.

[22] Gao, W., Mao, W., & Zhang, Z. (2021, February). Design of a high precision data acquisition system of weak signal. In Journal of Physics: Conference Series (Vol. 1815, No. 1, p. 012029). IOP Publishing.

[23] Deng, M., Deng, A., Zhu, J., & Sun, W. (2019). Adaptive bandwidth Fourier decomposition method for multi-component signal processing. IEEE Access, 7, 109776-109791.

[24] Wu, C., Tang, T., Elangage, J., & Krishnasamy, D. (2022). Accumulatively increasing sensitivity of ultrawide instantaneous bandwidth digital receiver with fine time and frequency resolution for weak signal detection. Electronics, 11(7), 1018.

[25] Elango, G. A., Sudha, G. F., & Francis, B. (2017). Weak signal acquisition enhancement in software GPS receivers–Pre-filtering combined post-correlation detection approach. Applied Computing and Informatics, 13(1), 66-78.

[26] Wang, P., Zhou, W., & Li, H. (2020). A singular value decomposition-based guided wave array signal processing approach for weak signals with low signal-to-noise ratios. Mechanical Systems and Signal Processing, 141, 106450.

[27] Chen, P., He, A., Zhang, T., & Dong, X. (2024). Weak vibration signal detection based on frequency domain cumulative averaging with DVS system. Optical Fiber Technology, 88, 103834.

[28] Liu, S., Sun, Y., He, L., & Kang, Y. (2022). Weak signal processing methods based on improved HHT and filtering techniques for steel wire rope. Applied Sciences, 12(14), 6969.

[29] Zhao, M., & Jia, X. (2017). A novel strategy for signal denoising using reweighted SVD and its applications to weak fault feature enhancement of rotating machinery. Mechanical Systems and Signal Processing, 94, 129-147.

[30] Zhang, G., Luo, J., Xu, H., Wang, Y., Wang, T., Lin, J., & Liu, Y. (2022). An improved UKF algorithm for extracting weak signals based on RBF neural network. IEEE Transactions on Instrumentation and Measurement, 71, 1-14.

[31] Song, H., Dong, H., & Zhang, P. (2017, May). A virtual instrument for diagnosis to substation grounding grids in harsh electromagnetic environment. In 2017 IEEE International Instrumentation and Measurement Technology Conference (I2MTC) (pp. 1-6). IEEE.

[32] Zhang, G., Xie, X., & You, Y. (2021). Multi-channel eddy current detector based on virtual instrument technology and self-balancing technology. Sensing and Imaging, 22(1), 12.

[33] Jiang, S., & Cheng, W. M. (2019, October). Motor temperature based on LoRa and virtual instrument Online monitoring system research. In 2019 3rd International Conference on Electronic Information Technology and Computer Engineering (EITCE) (pp. 398-401). IEEE.